

# On methods to determine bounds on the Q-factor for a given directivity

B.L.G. Jonsson, Shuai Shi, Lei Wang, Fabien Ferrero and Leonardo Lizzi

**Abstract**—This paper revisits the interesting case of bounds on the Q-factor for a given directivity for small antennas. Higher directivity in small antennas are closely connected with a narrow impedance bandwidth. The relation between bandwidth and a desired directivity is still not fully understood, not even for small antennas. Initial investigations in this direction has related the radius of a circumscribing spherical to the directivity, and bounds on the Q-factor has also been derived for a partial directivity in a given direction. In this paper we derive bounds on the Q-factor for a total desired directivity in a given direction as a convex problem using semi-definite relaxation techniques (SDR). SDR can also be used to relax a class of other interesting non-convex constraints in antenna optimization such as tuning, losses, front-to-back ratio. We compare two different new methods to determine the lowest Q-factor for a given total directivity. We also compare our results with full EM-simulations of a parasitic element antenna with high directivity.

## I. INTRODUCTION

Stored energy based physical bounds for arbitrarily shaped small antennas provide interesting and useful information about antenna design possibilities [1–3]. They set the outer boundaries of what is possible. Such information is helpful before starting the non-linear and complex process of designing antennas and as a benchmark on the antenna performance. The stored energy of an antenna determines the Q-factor which is closely related to the fractional impedance bandwidth performance of the antenna [9], [10]. To determine practical Q-factor bounds it is essential to also include the key desired constraints on the antenna design parameters. Such constraints can be on the far-field, tuning, front-to-back ratio, gain or on the directivity requirements.

However, only a small fraction of these and other constraints results in a convex optimization problem [1]. In this paper we show that we can formulate the bounds on the Q-factor for a total directivity in a given direction as a relaxed convex optimization problem. Indeed a large class of the non-convex constraint to Q-factor bounds can be relaxed into a convex problem. For the here investigated cases with constraints on the total directivity, it appears that the relaxed problems also give the solution to the original problems for small antennas. This is so far only shown by comparison with a non-linear solver, which is also described in the paper.

The relation between the antenna size and its maximal directivity has frequently been investigated, and it is known

that any directivity can be obtained given an aperture that supports high enough modes [4–6]. Harrington [7] used  $N$  spherical-modes to derive a limit for directivity as a function of size and Geyi [8] used Q-factors for spheres to obtain another limit for the directivity as function of the radius of an enclosing sphere. Beyond those spherical-shape based size-limitations, it is also well known that one can obtain bounds on the Q-factor for an arbitrary shaped antenna, for a given partial directivity [1]. However the extension of this latter bound to the total directivity results is a non-convex problem, and has thus been considered difficult to determine. The minimization problem can be formulated as a Euler-Lagrange equation with several Lagrange multipliers.

It is therefore very interesting that the semi-definite relaxation methods [11] enables us to obtain lower bounds for the Q-factor for this class of problems. Indeed this technique also allows us also to introduce other interesting non-convex constraints, like tuning and losses. The bound of [1] does not give size-limitation, but the lowest possible Q-factor for a given partial directivity. This work is in the same direction: find the lowest possible Q-factor bound for a given total directivity, in a desired direction. It rests on the observations [4–6] that any directivity is theoretically possible given a sufficiently high Q-factor. High enough Q-factors make such antenna solutions difficult to realize and to measure, it's thus more practically interesting to determine trade-offs between high directivity and as low as possible Q-factor. Earlier efforts in this direction has also been considered by *e.g.*, [1], [12], [13] in different contexts. We illustrate this type of lower Q-bounds for two types of shapes, and compare the results with a full-wave simulated highly-directive antenna. An overview of small antennas with high directivity can be found in [14].

There are advantages if the investigated optimization problem can be formulated as a convex problem: Such problems have a unique minimum, furthermore there are fast numerical methods to find both the minimum and minimizer see *e.g.*, [15]. These methods are so effective that sometimes the problem is considered ‘solved’ as soon as it has a convex formulation. This is not quite that straightly forward for antenna designs, but knowing bounds on the Q-factor certainly helps in defining antenna performance goals.

If the investigated constraint to the Q-factor optimization makes the problem non-convex, it is in general much harder to solve the problem. Tools like tracing multiple Lagrange parameters over some sub-domain see *e.g.*, [16], genetic algorithms and exhaustive searchers are in-general considerably slower and the problem might not have a unique minimum. In the case of Q-factor bounds we find that almost all constraints

B.L.G. Jonsson, Shuai Shi and Lei Wang are with KTH Royal Institute of Technology, at the School of Electrical Engineering, Stockholm, Sweden, e-mail: ljonsson@kth.se

F. Ferrero and L. Lizzi are with the University Cote d’Azur, CNRS, LEAT, Sophia Antipolis, France

Manuscript received Feb 10, 2017.

on the antenna parameters are linear or quadratic in the current density. This class of optimization problem is called quadratically constrained quadratic program (QCQP). It is known that this class includes NP-hard problems see *e.g.*, [11], and that this problem is in general not convex.

Successful convex methods to estimate a lower bound for the minimum of a QCQP problem are the semi-definite relaxation method (SDR) see *e.g.*, [11], [17] and the reformulation-linearization technique see *e.g.*, [18]. SDR, which is utilized in this paper, has recently been used to solve several interesting problems, ranging from beamforming in communication networks to phase-reconstruction [17], [19], [20]. SDR converts a QCQP-problem to a semi-definite programming problem see *e.g.*, [21]. The idea rests on a trace-operator identity that helps to reformulate the original problem into a linear relaxed problem. The original problem is thus formulated into an optimization of the trace of matrix products, usually also with constraints in terms of traces.

Trace-based methods provide a powerful tool to rewrite large classes of optimization problems. It has been shown that a class of data mining and machine learning problems can be formulated as trace-optimization problems in order to extract a set of small dimension out of a very large data sets see *e.g.*, [22]. This latter type of trace-optimization problems tends to be quadratic in their unknown, as a difference to the SDR problems investigated here. But it is interesting to observe how the trace is utilized to obtain a low-dimensional solution in both cases.

The numerical implementation of the relaxed problem gives a lower bound to the QCQP. The question naturally arises under what circumstances that the minimizer of the relaxed problem also solves the original numerical problem, for an overview of the distance between these two solutions see [17].

The rest of this paper consists of five sections. Section II defines the Q-factor and certain key antenna parameters. Section III formulates the minimization problems for the Q-factor with different directivity constraints and the use of the SDR technique. Section IV introduces a non-linear eigenvalue based method to estimate the minimum Q-factor, and Section V illustrates a few numerical examples, in which lower bounds on the Q-factor for the different methods are investigated. Comparison with a simulated high-directivity antenna is also illustrated. Section VI concludes the paper.

## II. ANTENNA TERMS

In this section we introduce the well known terms of directivity, gain and Q-factor for antennas see *e.g.*, [23], [29]. The aim is to precisely define the optimization problems that we study in the next section. Consider an antenna of finite extent placed in free space at the origin of our coordinate system. The antenna far-field radiation intensity  $U(\hat{\mathbf{r}})$  varies with the unit-direction  $\hat{\mathbf{r}}$  as seen from the center of the antenna. The total radiated power  $P_{\text{rad}}$  of the antenna is defined as

$$P_{\text{rad}} = \int_{S^2} U(\hat{\mathbf{r}}) d\Omega = \frac{1}{\eta} \lim_{R_0 \rightarrow \infty} \int_{|\mathbf{r}|=R_0} |\mathbf{E}|^2 dS \quad (1)$$

where  $S^2$  is the unit sphere in  $\mathbb{R}^3$ , and  $d\Omega = \sin\theta d\theta d\phi$  and  $dS = r^2 d\Omega$  and where we let  $\theta$  be the polar angle and

$\phi$  is the azimuth angle. Here  $\eta$  is the free space impedance. Given the currents densities on the antenna, we can directly determine its electric field  $\mathbf{E}$ , and hence its radiated power. Here  $\mathbf{r}$  is a vector in  $\mathbb{R}^3$  and  $r = |\mathbf{r}|$  with  $\hat{\mathbf{r}} = \mathbf{r}/r$ . It is often convenient to express the radiation intensity in terms of the far-field  $\mathbf{F}(\hat{\mathbf{r}})$  where  $r\mathbf{E}(\mathbf{r})e^{jkr} \rightarrow \mathbf{F}(\hat{\mathbf{r}})$  as  $r \rightarrow \infty$ . We have that  $U(\hat{\mathbf{r}}) = |\mathbf{F}(\hat{\mathbf{r}})|^2$ .

The total directivity,  $D(\hat{\mathbf{r}})$ , of an antenna is defined as the ratio of the radiation intensity in the direction  $\hat{\mathbf{r}}$  to the average radiation intensity,  $\bar{U}$ , over the sphere, *i.e.*,

$$D(\hat{\mathbf{r}}) = \frac{U(\hat{\mathbf{r}})}{\bar{U}} = \frac{4\pi U(\hat{\mathbf{r}})}{P_{\text{rad}}}, \quad (2)$$

and the peak total directivity is  $\max_{\hat{\mathbf{r}} \in S^2} D(\hat{\mathbf{r}})$ .

The gain  $G(\hat{\mathbf{r}})$  of an antenna accounts also for the efficiency  $\delta = P_{\text{rad}}/P_{\text{in}}$ , in the antenna where  $P_{\text{in}}$  is the input power to the antenna. The gain is defined as

$$G(\hat{\mathbf{r}}) = D(\hat{\mathbf{r}})\delta. \quad (3)$$

The partial gain, and the partial directivity are related to the directivity of a given polarization of the radiated field. That is consider a polarization-direction,  $\hat{\mathbf{e}}$ , orthogonal to the direction of observation direction  $\hat{\mathbf{r}}$ , then the partial directivity (partial-gain) is the radiation intensity in that polarization of the field *i.e.*,  $U(\hat{\mathbf{r}}, \hat{\mathbf{e}}) = |\hat{\mathbf{e}} \cdot \mathbf{F}(\hat{\mathbf{r}})|^2$  to the average radiated power (input power). In the present paper we will only consider loss-less antennas, *i.e.*,  $\delta = 1$ , where gain and directivity are equal, the reason for this limitation is that we are concerned here mainly with antennas of metal with very low losses. Indeed lossy antennas tend to have a larger bandwidth, and less radiated power due to the presence of Ohmic losses in the materials. Thus it is a tougher problem to obtain a large bandwidth in the loss-less case.

An interesting class of antennas are superdirective antennas see *e.g.*, [24]. It is well known that infinite directivity is possible [4–6]. Superdirectivity, is somewhat vaguely defined as antennas with above normal directivity. However, since the directivity is unbounded it is essential to compare at what cost the directivity comes. The essential feature here is bandwidth, since size does not necessarily limit directivity.

Small antennas tend to have low directivity due to their small size. However, higher directivity can also be obtained here at the expense of antenna bandwidth. An advantage with small antennas, *e.g.*, antennas with  $ka < 1$ , where  $k$  is the wave number and  $a$  is the radius of a sphere that circumscribe the antenna, are that the Q-factor gives an implicit way to define their relative bandwidth [9], [25]. The fractional (or relative) bandwidth  $B$  for a single resonance circuit is related to the Q-factor through the relation [9]:

$$B = \frac{f_2 - f_1}{f_0} \approx \frac{2\Gamma_0}{Q\sqrt{1 - \Gamma_0}}, \quad (4)$$

where the center frequency  $f_0 = (f_1 + f_2)/2$  and the magnitude of the maximally allowed reflection coefficient is  $\Gamma_0$ . When the input impedance of the antenna  $Z_{\text{in}} = R_{\text{in}} + jX_{\text{in}}$  is known one often define the impedance Q-factor through the relation [9], [25]

$$Q_Z = \frac{\sqrt{(\omega R'_{\text{in}})^2 + (\omega X'_{\text{in}} + |X_{\text{in}}|)^2}}{2R_{\text{in}}}. \quad (5)$$

A comparison between bandwidth and Q-factors for different definitions are given in [10].

The definition of the lower Q-bound for a loss-less antenna is defined as

$$Q = \min_{\mathbf{J}} \frac{\max(W_e(\mathbf{J}), W_m(\mathbf{J}))}{P_{\text{rad}}(\mathbf{J})}, \quad (6)$$

where  $\mathbf{J}$  is the current density on the antenna or on an extended body that encloses the antenna. Here  $W_e$  and  $W_m$  are the stored electric and the stored magnetic energy, defined below. Even for small antennas it is known that the Q-factor is not a perfect prediction of the fractional bandwidth, see [10], in which there is also comparisons between  $Q$  and  $Q_Z$  and their relation to the relative bandwidth. However, for Q-factors larger than  $\sim 5$  there is a fairly good correlation between high  $Q$  ( $Q_Z$ ) and the fraction bandwidth for small antennas.

Stored energies for antennas have been discussed thoroughly in the literature, see *e.g.*, [8–10], [26–35]. Here we use the definition:

$$W_e = W_e^{(0)} + W_{\text{em}}, \quad W_m = W_m^{(0)} + W_{\text{em}}, \quad (7)$$

where

$$W_e^{(0)} = \frac{\mu}{4k^2} \int_S \int_S (\nabla_1 \cdot \mathbf{J}_1)(\nabla_2 \cdot \mathbf{J}_2^*) \frac{\cos(k|\mathbf{r}_1 - \mathbf{r}_2|)}{4\pi|\mathbf{r}_1 - \mathbf{r}_2|} dS_1 dS_2, \quad (8)$$

$$W_m^{(0)} = \frac{\mu}{4} \int_S \int_S \mathbf{J}_1 \cdot \mathbf{J}_2^* \frac{\cos(k|\mathbf{r}_1 - \mathbf{r}_2|)}{4\pi|\mathbf{r}_1 - \mathbf{r}_2|} dS_1 dS_2, \quad (9)$$

and

$$W_{\text{em}} = \frac{-\mu}{4k} \int_S \int_S (k^2 \mathbf{J}_1 \cdot \mathbf{J}_2^* - (\nabla_1 \cdot \mathbf{J}_1)(\nabla_2 \cdot \mathbf{J}_2^*)) \frac{\sin(k|\mathbf{r}_1 - \mathbf{r}_2|)}{8\pi} dS_1 dS_2. \quad (10)$$

This definition is valid for non-magnetic material antennas. Stored energy for magnetic material antennas are investigated in [32], [34]. We have furthermore made the simplification that the current densities  $\mathbf{J}$  are surface current densities. Here we use the notation  $\mathbf{r}_1, \mathbf{r}_2 \in \mathbb{R}^3$ ,  $\mathbf{J}_1 = \mathbf{J}(\mathbf{r}_1)$  and similarly for  $\mathbf{J}_2$ ,  $\mu$  is the free space permeability. The surface  $S$  is the surface of the antenna structure, or a surface that enclose the structure.

The stored energies and the radiated power as well as the power intensity are determined numerically utilizing a Method of Moment (MoM) approach. Note that the stored energies are very similar to the components of the electric field integral equations, and it is thus easy to extract them from MoM codes. The in-house MoM-code is based on the Rao-Wilton-Glisson-basis functions and use a higher-order Gauss quadrature to determine the impedance matrix and DECDEM as described in [36] and references therein, for the singular terms. Utilizing the MoM-finite dimensional approximation of the electric field integral equations, we find that stored energy can be expressed as  $W_e \approx \langle I, \mathbf{w}_e I \rangle$ , where  $\mathbf{w}_e$  is a finite  $N \times N$ -matrix acting upon the current density coefficient vector  $I$ . Similarly, the radiated field is approximated by  $P_{\text{rad}} \approx \langle I, \mathbf{p}_r I \rangle$ . Here we use the notation  $\langle x, y \rangle = \sum_{n=1}^N x_n^* y_n$  as the inner product between

two vectors with  $N$ -elements. The electric far-field  $\mathbf{F}(\hat{\mathbf{r}})$  in a given polarization  $\hat{\mathbf{e}}$  and is approximated through  $\hat{\mathbf{e}} \cdot \mathbf{F}(\hat{\mathbf{r}}) \approx \langle f(\hat{\mathbf{r}}, \hat{\mathbf{e}}), I \rangle$ , where  $f$  is a vector. In the excellent tutorial [2] one can find a discussion on both a matrix formulation of key antenna terms as well as its application to convex optimization.

### III. BOUNDS ON THE Q-FACTOR

In this section we will formulate three different minimization problems towards the goal to determine a lower bound on the Q-factor for a given directivity-constraint. Lets start with the bounds on the Q-factor for a given partial directivity. In [1] they formulated the following  $D/Q$ -bound for superdirectivity, utilizing the observation that

$$D_0 < D(\hat{\mathbf{r}}, \hat{\mathbf{e}}) \approx \frac{4\pi |\langle f(\hat{\mathbf{r}}, \hat{\mathbf{e}}), I \rangle|^2}{2\eta \langle I, \mathbf{p}_r I \rangle}. \quad (11)$$

The maximum of the  $D/Q$  problem at  $D > D_0$  can be reformulated as a convex minimization problem:

$$\begin{aligned} & \text{minimize}_{I \in \mathbb{C}^N} \max(\langle I, \mathbf{w}_e I \rangle, \langle I, \mathbf{w}_m I \rangle) \\ & \text{subject to } \langle f(\hat{\mathbf{r}}, \hat{\mathbf{e}}), I \rangle = -j, \\ & \langle I, \mathbf{p}_r I \rangle \leq \frac{2\pi}{\eta D_0}. \end{aligned} \quad (12)$$

We refer to (12) as the  $D/Q$ -problem. Here  $\mathbb{C}^N$  is  $N$ -vectors with complex coefficients. Maximizing  $D/Q$  with constraints on  $D$ , naturally gives  $Q$  at a given  $D \geq D_0$ . However, we observe that the minimization reformulation of the problem does not state that we have obtained the peak partial directivity in the given direction  $\hat{\mathbf{r}}$ , only that the directivity in the desired direction is larger than  $D_0$ . The ingenious idea in [1] to formulate Q-factor bounds with a given partial directivity is easily solvable with cvx [15] or another convex-optimization solver given the respective matrices  $\mathbf{w}_e$ ,  $\mathbf{w}_m$  and  $\mathbf{p}_r$  together with the far-field vector  $f(\hat{\mathbf{r}}, \hat{\mathbf{e}})$ . The results yields both a minimizing current on the structure, as well as the unique minimum of the problem, see *e.g.*, [2].

If we instead want to formulate bounds for the Q-factor for the total directivity in the direction  $\hat{\mathbf{r}}$  we need to include both polarizations of the far-field *e.g.*,  $\hat{\mathbf{e}}$ ,  $\hat{\mathbf{h}}$ . Here  $(\hat{\mathbf{r}}, \hat{\mathbf{e}}, \hat{\mathbf{h}})$  forms a right-hand triple at each observation direction  $\hat{\mathbf{r}}$ . We note that  $|\langle f(\hat{\mathbf{r}}, \hat{\mathbf{e}}), I \rangle|^2 = \langle I, f(\hat{\mathbf{r}}, \hat{\mathbf{e}}) f^H(\hat{\mathbf{r}}, \hat{\mathbf{e}}) I \rangle$ . Lets introduce the matrix  $\mathbf{u}(\hat{\mathbf{r}}) = f(\hat{\mathbf{r}}, \hat{\mathbf{e}}) f^H(\hat{\mathbf{r}}, \hat{\mathbf{e}}) + f(\hat{\mathbf{r}}, \hat{\mathbf{h}}) f^H(\hat{\mathbf{r}}, \hat{\mathbf{h}})$ , which is related to the radiation intensity through  $U(\hat{\mathbf{r}}) \approx \langle I, \mathbf{u}(\hat{\mathbf{r}}) I \rangle / (2\eta)$ . The total directivity can hence be estimated through

$$D_* \leq D(\hat{\mathbf{r}}) \approx \frac{4\pi \langle I, \mathbf{u}(\hat{\mathbf{r}}) I \rangle}{2\eta \langle I, \mathbf{p}_r I \rangle}, \quad (13)$$

and we find the non-convex optimization problem to minimize the Q-factor with a given directivity

$$\begin{aligned} & \text{minimize}_{I \in \mathbb{C}^N} \max(\langle I, \mathbf{w}_e I \rangle, \langle I, \mathbf{w}_m I \rangle) \\ & \text{subject to } \langle I, \mathbf{p}_r I \rangle = 1, \\ & \langle I, \mathbf{u}(\hat{\mathbf{r}}) I \rangle \geq \frac{\eta}{2\pi} D_*. \end{aligned} \quad (14)$$

It is interesting to compare the solution to the lower Q-bounds in the respective case of (12) and (14), since it is not always

easy to predict which polarization that gives the lowest Q-factor. It depends both on the shape of the object, but also on the desired observation direction, see *e.g.*, Fig 1 in next section. The information that there are possible currents that provide a lower Q-factor if we relax our demand on the polarization is important, since the possibility of such currents that radiate part or all of its power in another polarization-direction will affect the antenna design. If polarization purity is important, then design measures to suppress the unwanted polarization may be required. However in *e.g.*, harvesting applications it is an advantage if multiple polarizations are absorbed by the antenna. Thus the cross-polarization levels are often an important factor in antenna designs.

The minimization problem given in (14) is non-convex, and has so far not been formulated as a convex optimization problem. The first observation is that the optimization problem fall in the category of quadratically constrained quadratic optimization programs (QCQP). Beyond the linear programming, quadratic programming is a rather well investigated class of optimization problems. QCQP-type problems are often occurring in physics applications where *e.g.*, energies are quadratic forms in terms of sources. There are several different methods to solve (14), either directly with a non-linear or heuristic solver or through a relaxation method. A powerful method to relax QCQP into convex problems is the semi-definite relaxation method (SDR). To derive the relaxed problem we follow the SDR-technique and observe that

$$\langle I, \mathbf{p}_r I \rangle = \text{tr}(I^H \mathbf{p}_r I) = \text{tr}(\mathbf{p}_r \mathbf{x}), \quad (15)$$

where  $\mathbf{x} = II^H$  is a rank 1 matrix and  $\text{tr}(\mathbf{x})$  is the trace of the matrix  $\mathbf{x}$ . With this observation we can now formulate the optimization problem for the lower Q-bound given a total directivity in the  $\hat{\mathbf{r}}$ -direction as

$$\begin{aligned} & \underset{\mathbf{x} \in \mathbb{C}^{N \times N}, \mathbf{x} \succeq 0}{\text{minimize}} && \max(\text{tr}(\mathbf{w}_e \mathbf{x}), \text{tr}(\mathbf{w}_m \mathbf{x})) \\ & \text{subject to} && \text{tr}(\mathbf{p}_r \mathbf{x}) = 1, \\ & && \text{tr}(\mathbf{u}(\hat{\mathbf{r}}) \mathbf{x}) \geq \frac{\eta}{2\pi} D_*, \end{aligned} \quad (16)$$

where we have dropped, relaxed, the rank  $\mathbf{x} = 1$  condition in order to make the problem convex. The problem (16) falls in the class of semi-definite programming, and there are efficient methods to solve rather large such problems see *e.g.*, [37].

If we compare these different minimization problems for bounds the Q-factor we note that both (12) and (16) are convex and hence each has a unique minimum. However (16) has a much larger set of unknowns in its  $N \times N$ -matrix  $\mathbf{x}$  that is positive semi-definite, as compared with, the  $N$ -vector of  $I$ . We thus tend to obtain rather large minimization problems for (16). The relaxed problem (16) will always be a lower bound to the original problem (14). However, as we will see below we find that it well predicts the solution to (14) in all observed cases. An associated effect of the relaxed problem is that the desired solution  $\mathbf{x}$  might not be a rank one matrix. There are several methods to extract feasible rank one solutions, see *e.g.*, [17].

Above we have focused on the total directivity. We note in passing that several of other desirable constraints like

antenna tuning requiring  $W_e = W_m$ , losses, and other far-field constraints can also be formulated as relaxed convex problems since they all fall in the category of quadratically constrained quadratic programming. See also [38], [39].

#### IV. A HEURISTIC GENERALIZED EIGENVALUE-APPROACH TO Q-FACTOR BOUNDS

In this section we introduce an alternative method to determine the lower bounds on the Q-factor for a total directivity (14). We will use this latter method to compare how well a solution to the relaxed problem (16) estimates the solution to the original problem (14). We also use this method to solve problems where the memory demands of solution methods to (16) become too large. It was observed in [2] that for  $\alpha \in [0, 1]$

$$\max(\langle I, \mathbf{w}_e I \rangle, \langle I, \mathbf{w}_m I \rangle) \geq \langle I, (\alpha \mathbf{w}_e + (1 - \alpha) \mathbf{w}_m) I \rangle, \quad (17)$$

which was used in [3] to show that the duality gap for Q-factors are tight, *i.e.*, that  $\mathbf{w}_\alpha = \alpha \mathbf{w}_e + (1 - \alpha) \mathbf{w}_m$  can be used in a generalized eigenvalue problem to determine the Q-factor bound without any constraints. That is the problem

$$\begin{aligned} & \underset{I}{\text{minimize}} && \langle I, \mathbf{w}_\alpha I \rangle \\ & \text{subject to} && \langle I, \mathbf{p}_r I \rangle = 1, \end{aligned} \quad (18)$$

can be formulated as a generalized eigenvalue problem  $\mathbf{w}_\alpha I = \lambda_\alpha \mathbf{p}_r I$ . Lower bounds on  $Q$  are shown in [3] to be equal to  $Q = \max_\alpha \min_{n \in N} \lambda_{\alpha, n}$ . Certain care has to be applied numerically since the matrix  $\mathbf{p}_r$  can fail to be numerically positive definite even though  $P_{\text{rad}} > 0$ . This is associated with that  $\mathbf{p}_r$  is a low rank matrix corresponding to the propagating vector spherical modes of the antenna, for a discussion see [2].

To generalize (18) to include constrains on the total directivity is straight forward. The Lagrangian associated with (14), after using (17) is

$$\mathcal{L} = \langle I, [\mathbf{w}_\alpha - \lambda(\mathbf{p}_r - 1) + \sigma(\mathbf{u}(\hat{\mathbf{r}}) - \frac{\eta D_*}{2\pi})] I \rangle. \quad (19)$$

The Euler-Lagrange equations, *i.e.*, critical points to (19) are solutions to the generalized eigenvalue problem

$$(\mathbf{w}_\alpha + \sigma \mathbf{u}(\hat{\mathbf{r}})) I = \lambda \mathbf{p}_r I. \quad (20)$$

One heuristic method to find solutions to this problem could consist of the following steps:

- Fix the parameters  $\alpha$  and  $\sigma$  and determine all generalized eigenvalues of  $\lambda_n$  and its associated eigenvectors  $I_n$ .
- Sweep  $\alpha \in [0, 1]$  and  $\sigma \in \mathbb{R}$  to find the smallest feasible solution for a given  $(\alpha, \sigma, \lambda, I)$ .

It is an exhausting (slow) search for the appropriate minimum due to both large  $N$  but also that the eigenvalue problem has to be solved a large number of times to trace out the feasible space in the parameters  $(\alpha, \sigma)$ . Certain care has to be take, given the additional parameter  $\sigma$  as compared to the problem given in (18), since  $\sigma$  corresponds to the directivity constraint. Thus even though the bound on the relaxed Q-factor given in (18) yields the Q-factor, this is not clear that this is the case in solutions to (20). That is the best  $\lambda$  does not necessarily

give the smallest  $Q$ -factor, or to formulate it differently, there might be a duality gap.

Clearly any current  $I$  inserted in the original problem (14) is an upper approximation of the lowest bound. A heuristic approach followed here to find the lowest possible bound is as follows:

- Utilize solutions  $(\lambda_n, I_n)$  to the generalized eigenvalue problem given in (20) for a particular  $\alpha, \sigma$ .
- Select the sub-set of feasible solutions, *i.e.*, these that satisfies the minimal directivity constraints. Test which of these ones give the smallest  $Q$ -factor in (14).
- Repeat the above procedure for a new sample of  $(\alpha, \sigma)$ .
- After an exhaustive search over some grid of the  $(\alpha, \sigma)$ -space, we use the best solution as an initial point in matlab's `fminsearch` over  $\alpha, \sigma$  to further approach the minimum.

The method is rather slow, however we can speed it up by noticing that both  $\mathbf{u}$  and  $\mathbf{p}_r$  are of low rank, which substantially reduces the set of eigenvalues that needs to be investigated at each  $(\alpha, \sigma)$ .

## V. NUMERICAL EXAMPLES – Q-FACTOR BOUNDS FOR SUPERDIRECTIONAL ANTENNAS

Small antennas with higher than normal directivity are particularly interesting for internet-of-things (IoT) applications where the expected bandwidth of the device is very narrow. As an example, in Europe, the entire ISM-band at 900 MHz has a relative bandwidth of 2.8% corresponding to a half-power  $Q$ -factor at 70. The ISM-band at 868 MHz has an even smaller bandwidth. Moreover, most of the applications are only using a 1 MHz BW-channel since the amount of data to be transmitted is very limited *e.g.*, for a physical parameter monitored by a sensor or the location coordinates calculated by a GPS receiver. Thus, even higher  $Q$ -factor might be feasible for IoT applications. High gain of small devices may enable them to communicate at a lower power-level, which is essential to reduce the power consumption in their communication mode, and hence save battery or harvested energy. High directivity can also be utilized to reduce interference with neighboring devices, which is essential to reduce packet collision and avoid the retransmission process [40], thus saving on the power resources at both the device and network level. Moreover, for wearable applications, directive antennas are more efficient since they reduce the energy absorbed by the body.

### A. Single plate structure

In the example depicted in Fig. 1 we sweep the  $\hat{\mathbf{r}}(\theta, \phi)$ -direction for the polar angle  $\theta \in [0^\circ, 90^\circ]$  and  $\phi = 0^\circ$ . We determine the optimal currents on an infinitesimally thin rectangle of size 32mm  $\times$  44mm located in the  $xy$ -plane, at the frequency  $f = 900$  MHz, see the insert in Fig. 1. We compare the result between the problem (12) for  $\hat{\mathbf{e}} = \hat{\boldsymbol{\varphi}} = \hat{\mathbf{y}}$  and the trace- $Q$  minimization (16) that allows both polarizations. We find that the trace-minimization has a lower  $Q$ -bound for  $\theta \leq 10^\circ$  as compared with the  $D/Q$ -calculation, in particular for  $D > 2.1$  and  $D > 2.5$  (dBi) respective for  $\theta = 0^\circ$  and  $\theta = 10^\circ$ . At the investigated directions with  $\theta \geq 20^\circ$ , we

note that the trace-optimization and the  $D/Q$  optimization largely agree. One feature of the trace-minimization is that it allows solutions with rank 2 that can have considerably lower directivity, as illustrated with the flat start on the  $\theta = 90^\circ$  curve with trace-minimization. The non-linear eigenvalue calculation agrees with the trace-minimization problem. Thus we have established that in the investigated case we do not only obtain a lower estimate of the  $Q$ -value, but the solution to the optimization problem (14). The envelope that consists of  $(ka)^3 Q = 4.6$  for  $D < 3.5$ , combined with the  $\theta = 90^\circ$ -curve is an estimate of the lower range of the bound of the  $Q$ -factor as a function of the total directivity.

As always in this kind of simulations it is possible to increase the resolution and thus decrease the minimal  $Q$ -value to a small extent. In the present calculation we have used a  $10 \times 14$  regular grid on the rectangle, resulting in an impedance matrices with  $\sim 400 \times 400$  elements.

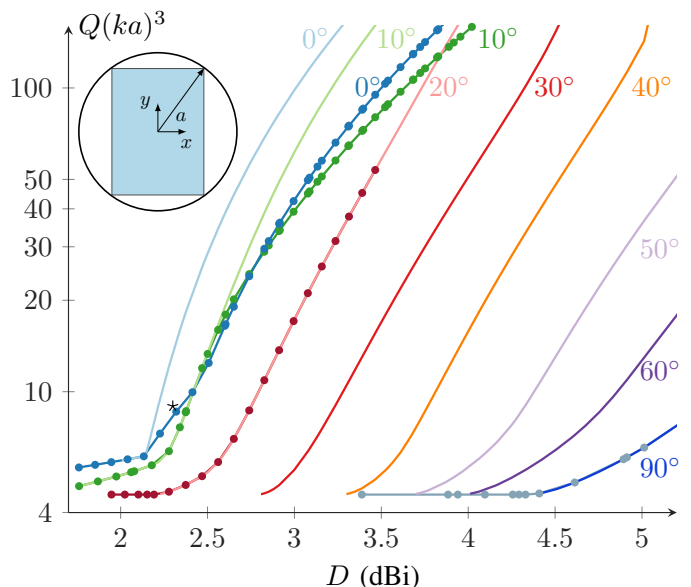


Fig. 1. Comparison between  $D/Q$ -optimization (12) and trace-optimization (16). The trace-optimization curves are lines marked with small dots and are depicted above for  $\theta \in [0^\circ, 10^\circ, 20^\circ, 90^\circ]$ . For  $\theta \in [20^\circ - 90^\circ]$  both minimizations yield the same minimum in the considered  $Q$ -range, apart from that the trace-minimization find solutions also for lower directivity, as is indicated by the horizontal-tail of  $\theta = 90^\circ$  in light blue, in the lower right-hand corner of the graph. The star at  $D = 2.3$  dBi is a full wave simulation ( $D, Q_z$ ) at 855 MHz of one of the elements depicted in Fig. 5. The  $(ka)^3$  scaling of  $Q$  allows us to compare results for frequencies where the antenna is small. See *e.g.*, the comparisons of  $D/Q$  for different frequencies in Fig. 4.

### B. Two plate structure

In our second example, we consider two rectangular plates of 32mm  $\times$  44mm, parallel to the  $xy$ -plane and with a distance between them of 40mm along the  $z$ -axis, see Fig. 2. The optimization sets a direction  $\hat{\mathbf{r}}(\theta, \phi)$ , and we sweep  $\theta \in [0^\circ, 90^\circ]$ . The directional constraints in the optimization is not equivalent with that the peak directivity is in that direction, as mentioned above. To illustrate this we utilize the convex minimization in (12) at the lowest possible  $D$  for the  $\hat{\mathbf{r}}(\theta, \phi)$

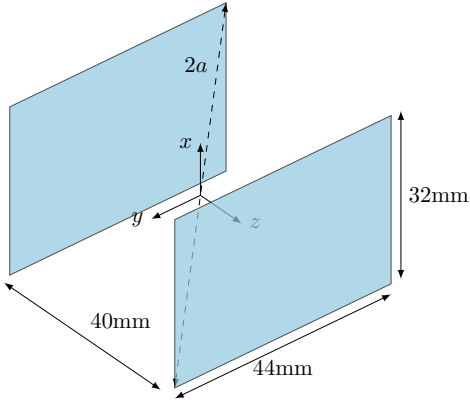


Fig. 2. The antenna enclosing structure used in the second example, see Fig. 3 and Fig. 4.

angles  $\theta \in [0^\circ, 36^\circ, 63^\circ, 90^\circ]$ . The radiation pattern in the  $xz$ -plane with a  $y$ -polarized field correspond to the lowest  $Q$ -value for each of these angles are depicted in red in Fig. 3. The blue radiation patterns corresponds to the same angles, but now at directivity  $D \approx 5.4$  dBi. The realized radiation pattern at the two intermediate angles do not have their peak directivity at the aimed for angles of  $36^\circ$  and  $63^\circ$  respectively. We note that the optimization does not require that the peak directivity is in the direction of  $\hat{r}$ . However, as the directivity becomes larger, we see that the main peak-direction approaches the desired angle. See Fig. 3b, and 3c, where the peak of the blue line moves towards the goal  $\hat{r}$ -direction.

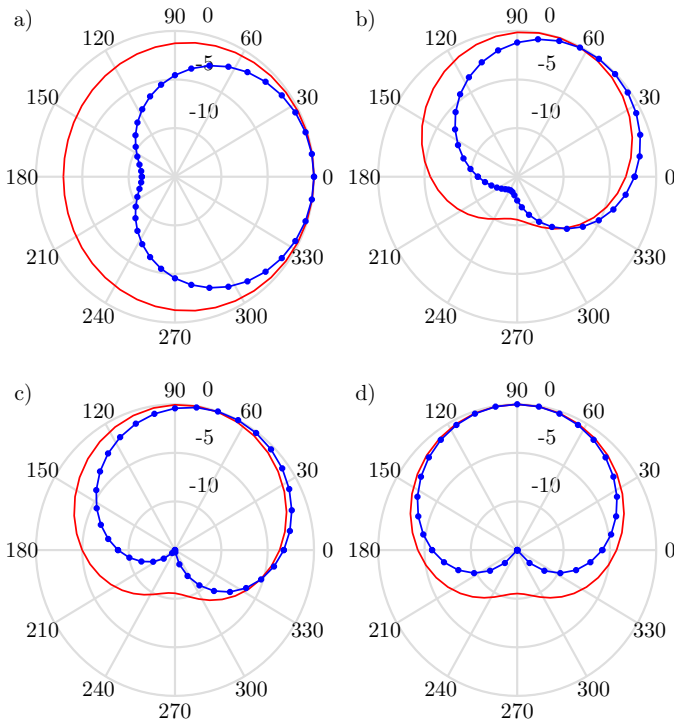


Fig. 3. The normalized radiation patterns in figure [a,b,c,d] corresponds to a  $\hat{r}$ -goal direction of  $[0^\circ, 36^\circ, 63^\circ, 90^\circ]$ . The red line corresponds to the lowest  $D$ -value possible in the  $D/Q$ -optimization (12), that is points on the lowest value of the (12)-minimization (green line) in Fig. 4. The blue lines, with dots are currents where  $D(\hat{r}) = D_0 \approx 5.4$  dBi for the same desired  $\hat{r}$ -angles.

In Fig. 3b, at the lowest  $Q$ -value (the red curve) we find that the peak radiation direction is  $\approx 70^\circ$ , instead of the expected  $36^\circ$ . Our interpretation of this solution to the minimization problem (12) is that the current minimizer consists mainly of a current with low- $Q$  radiation at  $90^\circ$  perturbed by a current that ensures that the direction  $36^\circ$  has large enough far-field amplitude. These currents are scaled in such a way so that the constraints are satisfied. The interpretation is hence that it is more costly in  $Q$ -factor (smaller bandwidth) to have the peak direction to  $36^\circ$  than it is to scale up a slightly perturbed radiation pattern at  $90^\circ$ . By increasing the demands on  $D_0$  to  $D \approx 5.4$  dBi we find that the  $Q$ -factor also increases, see Fig. 4. This ensures that it costs more in  $Q$ -factor to use a peak directivity in another direction, since high directivity amounts to less radiation in non-peak directions. This is also indicated with the blue line in Fig. 3b white where the peak direction moves more towards  $36^\circ$ . We see the same phenomena for a desired peak direction at  $63^\circ$  in Fig. 3c.

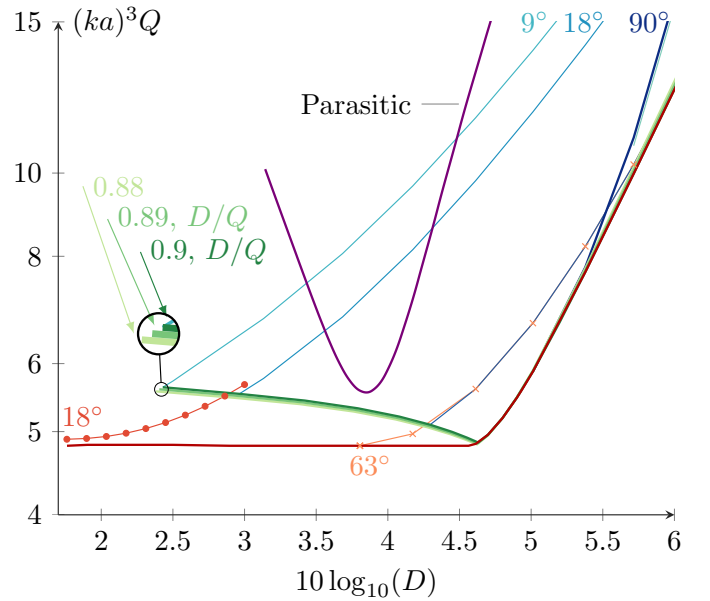


Fig. 4. Comparison between  $D/Q$ -optimization (12), trace-optimization (16) and non-linear eigenvalue search (14). The trace-optimization curves are marked with small dots and are depicted above for  $\theta = 18^\circ$  and  $N = 7$  (orange). The  $D/Q$ -case are sampled in blueish colors for  $\theta \in [9^\circ, 18^\circ, 63^\circ, 90^\circ]$ , and  $N = 10 \times 14$ . The non-linear eigenvalue search is included for  $\theta = 63^\circ$ . It also defines the dark-red envelope at the bottom of the figure corresponding to the lowest  $Q$  sweeping  $\theta \in [0^\circ, 90^\circ]$ . The green-hue colors corresponds to the envelope of the lowest  $Q$ -values from the  $D/Q$ -optimization for frequencies  $[0.88, 0.89, 0.90]$  GHz. The line marked parasitic corresponds to a Parasitic element antenna, see Fig. 5.

The  $D/Q$ -calculations are depicted in blueish in Fig. 4. The smallest in  $Q$ -factor envelope over all  $D/Q$  calculations upon sweeping over the desired observation direction  $\theta$  is shown in green. The green lines consists of the frequencies  $f = [0.88, 0.89, 0.90]$  GHz. Due to the  $(ka)^3$ -normalization we find that they essentially are one line, showing that the electric polarization is essential in determining these  $Q$ -bounds. The red envelope in Fig. 4 is the smallest  $Q$  in solving (14) using the non-linear eigenvalue method. For  $Q$ -values that is larger than the green line, we have that the lowest  $Q$ -value for (12) and (14) agree, as illustrated with  $\theta = 63^\circ$ .



case. The mesh used in this case is the same as the mesh for one rectangle, *i.e.*,  $N = 10 \times 14$  for each rectangle. To investigate the sensitivity to increasing the mesh we also have used  $N = 15 \times 21$ , with only a few points that are inserted below and almost coinciding with the line for  $\theta = 90^\circ$  up in the right corner of the figure (light blue). Comparing with solutions to the trace-problem is harder in this case. Solutions with  $N = 5 \times 7$  and  $N = 7 \times 10$  fill the region between the red and the green line, with small perturbations, as illustrated with the  $\theta = 18^\circ$  for  $N = 7 \times 10$ . To illustrate a bit of the challenge in solving the  $N = 10 \times 14$ -case with *cvx*, we find that the SeDuMi solver converts and solves the problem of size dimension  $\sim 3 \cdot 10^5$  for the  $N = 7 \times 10$ -case, whereas the  $N = 10 \times 14$  correspond to a problem of size  $1.2 \cdot 10^6$ . This rapid growth limits the size of the investigated problems. However we note that a comparison between the speed of the trace-optimization and the non-linear eigenvalue search shows that the trace-method is faster. Thus given sufficient memory, trace is an attractive method. We once again observe that the trace-bounds on  $Q$  seems to be tight, *i.e.*, they are also solutions to (14).

Another phenomena that is illustrated in Fig. 4 is that the lowest possible  $Q$ -factor for a particular directivity is not necessarily one with radiation in a cardinal direction. Note that at  $D > 5.3$  dBi we see that the curve marked  $90^\circ$  has a higher  $Q$ -value than the curve marked  $\theta = 63^\circ$ . In Fig. 3c we have that the blue line have its peak directivity at  $\approx 63^\circ$ . Similarly the blue radiation pattern with  $D \approx 5.4$  dBi in Fig. 3d has its peak at  $90^\circ$ . Thus an interpretation is that as we solve the minimization problem with higher requirement on the directivity, we find current minimizers also with non-cardinal peak radiation direction with a lower  $Q$ -factor than currents that radiate in the cardinal direction. It is nice to see how this process still smoothly trace out the lower- $Q$  envelope as a function of  $D$  given by the low- $Q$  red line in the graph. In essence, we find that depicted curve furthestmost to the right (red) is a description of the lowest  $Q$ -factor increase with demands on directivity. The red line thus describe the cost in  $Q$ -factor for a desired (super)directivity.

In Fig. 4 we have also included a lilac curve marked ‘Parasitic’ that corresponds to a full-wave simulation of a high-directivity parasitic element antenna of the shape shown in Fig 5. The shape fits into the investigated double-rectangle structure. It is composed with a driven element (upper plate) and a parasitic element (lower plate). It is closely related to a realized and measured antenna, discussed in [41]. We see that the lowest point of the parasitic curve comes rather close to the low green  $D/Q$ -line *e.g.*, it has a fairly high directivity, while keeping the  $Q$ -factor low. If it is possible to realize antennas on the green, or even better closer the red marked lower  $Q$ -factor envelope in (4) is still an open question.

## VI. CONCLUSION

We show that semi-definite relaxation can be used to determine the  $Q$ -factor for a given total directivity. Often it agrees with the  $Q$ -bounds for a given partial directivity. However, in the two illustrated cases we also note that there are cases with

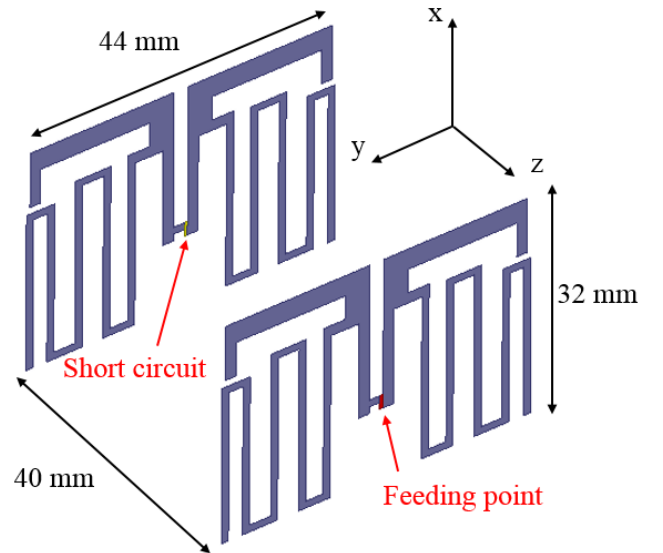


Fig. 5. EM Model of the two plates parasitic superdirective antenna.

lower  $Q$ -factors if we allow for both polarizations. The reason that we use the lowest  $Q$ -factor to bound (super)directivity is that size does not necessarily limit the directivity. However, as we have illustrated, given a desired  $Q$ -factor, there is a limited maximal directivity. Thus by connecting directivity to its maximally allowed  $Q$ -factor for a given shape, we find an approximation to the widest bandwidth associated with a desired total directivity. Another observation is that for the investigated cases we find that the semi-definite relaxation method seems to give tight bounds on the original quadratically constrained problem of determining the lowest  $Q$ -factor at a given total directivity  $D(\hat{r})$ .

## ACKNOWLEDGEMENTS

LJ and FF are grateful to the Labex UCN@Sophia for having funded Lars Jonsson visiting period in University Nice Sophia. LJ gratefully acknowledge the support from the Swedish foundation for strategic research for the project ‘‘Convex analysis and convex optimization for EM design’’, and LJ and LW gratefully acknowledge the support from Swedish Governmental Agency for Innovation Systems through the center ChaseOn in the project iAA. SS gratefully acknowledge funding from CSC.

## REFERENCES

- [1] M. Gustafsson and S. Nordebo, ‘‘Optimal antenna currents for  $Q$ , superdirectivity, and radiation patterns using convex optimization,’’ *IEEE Trans. Antennas Propagat.*, vol. 61, no. 3, pp. 1109–1118, 2013.
- [2] M. Gustafsson, D. Tayli, C. Ehrenborg, M. Cismasu, and S. Nordebo, ‘‘Antenna current optimization using MATLAB and CVX,’’ *FERMAT*, vol. 15, no. 5, pp. 1–29, 2016.
- [3] M. Capek, M. Gustafsson, and K. Schab, ‘‘Minimization of antenna quality factor,’’ *ArXiv e-prints*, 1612.0767, 2016. [Online]. Available: <http://arxiv.org/abs/1612.0767>
- [4] A.I. Uzkov, ‘‘An approach to the problem of optimum directive antennae design,’’ *Comptes rendus (Doklady) de l’Academie des Sciences de l’URSS*, vol. 53 no. 1 pp. 3538, 1946.

- [5] H.J. Riblet, "Note on the maximum directivity of an antenna," Proc. IRE, vol. 36 pp. 620624, 1948.
- [6] R.C. Hansen, "Fundamental limitations in antennas," Proc. IEEE, vol. 69, no. 2, pp. 170182, 1981.
- [7] R.F. Harrington, "On the gain and beamwidth of directional antennas," IRE Trans. Antennas Propag., vol. 6 pp. 219225, 1958.
- [8] W. Geyi, "Physical limitations of antenna," *IEEE Trans. Antennas Propagat.*, vol. 51, no. 8, pp. 2116–2123, Aug. 2003.
- [9] A. D. Yaghjian and S. R. Best, "Impedance, bandwidth, and  $Q$  of antennas," *IEEE Trans. Antennas Propagat.*, vol. 53, no. 4, pp. 1298–1324, 2005.
- [10] M. Gustafsson and B. L. G. Jonsson, "Antenna  $Q$  and stored energy expressed in the fields, currents, and input impedance," *IEEE Trans. Antennas Propagat.*, vol. 63, no. 1, pp. 240–249, 2015.
- [11] M. X. Goemans and D. P. Williamson, "Improved approximation algorithms for maximum cut and satisfiability problems using semidefinite programming," *Journal of the ACM (JACM)*, vol. 42, no. 6, pp. 1115–1145, 1995.
- [12] Y. T. Lo, S. W. Lee, and Q. H. Lee. "Optimization of directivity and signal-to-noise ratio of an arbitrary antenna array," *Proceedings of the IEEE*, vol. 54 no. 8 pp. 1033-1045, 1968.
- [13] D. Margetis, G. Fikioris, J. Myers, and T. Wu, "Highly directive current distributions: General theory," *Phys. Rev. E*, vol. 58, no. 2, p. 2531–2547, 1998.
- [14] M. Pigeon, C. Delaveaud, L. Rudant and K. Belmkaddem, "Miniature directive antennas," *International Journal of Microwave and Wireless Technologies*, vol. 6 no. 1 pp. 45-50, 2014.
- [15] M. Grant and S. Boyd, "CVX: Matlab software for disciplined convex programming, version 2.1," [cvxr.com/cvx](http://cvxr.com/cvx), Apr. 2014.
- [16] L. Jelinek and M. Capek, "Optimal currents on arbitrarily shaped surfaces," *IEEE Trans. Antennas Propag.*, vol. 65, no. 1, p. 329341, 2017.
- [17] Z.-Q. Luo, W.-K. Ma, A. M.-C. So, Y. Ye, and S. Zhang, "Semidefinite relaxation of quadratic optimization problems," *IEEE Signal Processing Magazine*, vol. 27, no. 3, pp. 20–34, 2010.
- [18] K. M. Anstreicher, "Semidefinite programming versus the reformulation-linearization technique for nonconvex quadratically constrained quadratic programming," *Journal of Global Optimization*, vol. 43, no. 2-3, pp. 471–484, 2009.
- [19] M. Bengtsson and B. Ottersten, "Optimal and suboptimal transmit beamforming," in *Handbook of Antennas in Wireless Communications*. CRC Press, 2001, pp. 18–1.
- [20] E. J. Candes, Y. C. Eldar, T. Strohmer, and V. Voroninski, "Phase retrieval via matrix completion," *SIAM review*, vol. 57, no. 2, pp. 225–251, 2015.
- [21] L. Vandenberghe and S. Boyd, "Semidefinite programming," *SIAM review*, vol. 38, no. 1, pp. 49–95, 1996.
- [22] E. Kokiopoulou, J. Chen, and Y. Saad, "Trace optimization and eigenproblems in dimension reduction methods," *Numerical Linear Algebra with Applications*, vol. 18, no. 3, pp. 565–602, 2011.
- [23] C. A. Balanis, *Antenna Theory*, 3rd ed. New Jersey: John Wiley & Sons, 2005.
- [24] R. C. Hansen, *Electrically Small, Superdirective, and Superconductive Antennas*. New Jersey: John Wiley & Sons, 2006.
- [25] M. Gustafsson and S. Nordebo, "Bandwidth,  $Q$ -factor, and resonance models of antennas," *Progress in Electromagnetics Research*, vol. 62, pp. 1–20, 2006.
- [26] R. E. Collin and S. Rothschild, "Evaluation of antenna  $Q$ ," *IEEE Trans. Antennas Propagat.*, vol. 12, pp. 23–27, Jan. 1964.
- [27] R. L. Fante, "Quality factor of general antennas," *IEEE Trans. Antennas Propagat.*, vol. 17, no. 2, pp. 151–155, Mar. 1969.
- [28] D. M. Pozar, "New results for minimum  $Q$ , maximum gain, and polarization properties of electrically small arbitrary antennas," in *Antennas and Propagation, 2009. EuCAP 2009. 3rd European Conference on*, March 2009, pp. 1993–1996.
- [29] G. A. E. Vandenbosch, "Reactive energies, impedance, and  $Q$  factor of radiating structures," *IEEE Trans. Antennas Propagat.*, vol. 58, no. 4, pp. 1112–1127, 2010.
- [30] M. Gustafsson, M. Cismasu, and B. L. G. Jonsson, "Physical bounds and optimal currents on antennas," *IEEE Trans. Antennas Propagat.*, vol. 60, no. 6, pp. 2672–2681, 2012.
- [31] M. Capek, Jelinek, L., Hazdra, P., and J. Eichler, "The measurable  $Q$  factor and observable energies of radiating structures," *IEEE Trans. Antennas Propagat.*, vol. 62, no. 1, pp. 311–318, 2014.
- [32] B. L. G. Jonsson and M. Gustafsson, "Stored energies in electric and magnetic current densities for small antennas," *Proc. R. Soc. A*, vol. 471, no. 2176, p. 20140897, 2015.
- [33] M. Capek and L. Jelinek, "Various Interpretations of the Stored and the Radiated Energy Density," *ArXiv e-prints*, Mar. 2015.
- [34] B. L. G. Jonsson and M. Gustafsson, "Stored energies for electric and magnetic current densities," arXiv:1604.08572, pp. 1–25, 2016.
- [35] M. Capek, L. Jelinek, and G. Vandenbosch, "Stored electromagnetic energy and quality factor of radiating structures," *Proc. R. Soc. A*, vol. 472, no. 2188, p. 201604, 2016.
- [36] A. G. Polimeridis and J. R. Mosig, "On the direct evaluation of surface integral equation impedance matrix elements involving point singularities," *IEEE Antennas Wireless Propag. Lett.*, vol. 10, pp. 599–602, 2011.
- [37] B. O'Donoghue, E. Chu, N. Parikh, and S. Boyd, "Conic optimization via operator splitting and homogeneous self-dual embedding," *Journal of Optimization Theory and Applications*, vol. 169, no. 3, pp. 1042–1068, June 2016. [Online]. Available: <http://stanford.edu/~boyd/papers/scs.html>
- [38] S. Shi, L. Wang, and B. L. G. Jonsson, "On  $Q$ -Factor Bounds for a Given Front-to-Back Ratio," submitted Jan. 2017.
- [39] B.L.G. Jonsson, S. Shi and L. Wang, "Relaxation of some non-convex constraints for  $Q$ -factor optimization", submitted as a conference abstract, Jan, 2017.
- [40] T. N. Le et al., "Improving energy efficiency of mobile WSN using reconfigurable directional antennas," *IEEE Communications Letters*, vol. 20, no. 6, pp. 1243–1246, 2016.
- [41] F. Ferrero and L. Lizzi, "Super-directive parasitic element antenna for spatial filtering applications," 2016 IEEE International Symposium on Antennas and Propagation (APSURSI), Fajardo, 2016, pp. 1753-1754.